Multistream Heat Exchangers: Equation-Oriented Modeling and Flowsheet Optimization

Richard C. Pattison and Michael Baldea
McKetta Dept. of Chemical Engineering, The University of Texas at Austin, Austin, TX 78712

DOI 10.1002/aic.14766
Published online March 21, 2015 in Wiley Online Library (wileyonlinelibrary.com)

Multistream heat exchangers (MHEXs), typically of the plate-fin or spiral-wound type, are a key enabler of heat integration in cryogenic processes. Equation-oriented modeling of MHEXs for flowsheet optimization purposes is challenging, especially when streams undergo phase transformations. Boolean variables are typically used to capture the effect of phase changes, adding considerable difficulty to solving the flowsheet optimization problem. A novel optimization-oriented MHEX modeling approach that uses a pseudo-transient approach to rapidly compute stream temperatures without requiring Boolean variables is presented. The model also computes an approximate required heat exchange area to determine the optimal tradeoff between operating and capital expenses. Subsequently, this model is seamlessly integrated in a previously-introduced pseudo-transient process modeling and flowsheet optimization framework. Our developments are illustrated with two optimal design case studies, an MHEX representative of air separation operation and a natural gas liquefaction process. © 2015 American Institute of Chemical Engineers *AIChE J*, 61: 1856–1866, 2015
Keywords: optimization, design (process simulation), mathematical modeling

Introduction

Tight heat integration is essential to the economic success of modern chemical processes.[1] Extensive efforts have focused on methods for finding the optimal structure of the heat exchange network (HEN) of a process, either in retrofits or for new designs.[2–4] Several processes (e.g., natural gas liquefaction, air separation, food manufacturing) call for the use of multistream heat exchangers (MHEXs) for achieving optimal heat integration. MHEXs facilitate thermal contact between multiple hot and cold streams in a single unit. Typically, plate-fin type or spiral-wound MHEXs are preferred in such processes because their compact designs allow for minimal driving forces (i.e., low-temperature differences between the hot and cold streams) and afford substantial heat recovery.[5] Figure 1 shows an example MHEX connected to a process flowsheet.

Modeling and optimization of process flowsheets that make use of MHEXs require accurate models which robustly account for phase transitions and the change of physical properties over wide temperature ranges. Such models must be capable of finding a high-level design target for the MHEX while simultaneously selecting the optimal operating conditions throughout the flowsheet. Heat exchanger designs must (1) ensure that the unit operation is thermodynamically feasible, that is, the required heat can be exchanged between the hot and cold process streams while maintaining a minimum temperature driving force along the entire heat exchanger, and (2) find the heat-transfer parameters (the product of area and the heat-transfer coefficient) (UA) necessary to achieve the prescribed heat duty.

In this work, we develop a robust equation-oriented (EO) modeling and optimization framework for MHEXs for flowsheet optimization applications. First, we describe our previously developed pseudo-transient EO flowsheet simulation and optimization framework, followed by a description of the challenges associated with developing robust and computationally tractable EO MHEX models. Next, we give a brief overview of the literature relevant to dealing with phase changes in HEN and MHEX design optimization. Then, a complete description of our novel modeling methodology for MHEXs is provided, and we further discuss the approach in the context of flowsheet optimization. Finally, two case studies are modeled and optimized, an MHEX representative for the operation of air separation units, and an industrial gas liquefaction process.

Background

Pseudo-transient process modeling

In our previous work,[6,7] we developed a library of EO models of common unit operations (reactors, flash tanks, distillation columns, compressors, two-stream heat exchangers, etc.) that use pseudo-transient continuation methods[8] to solve the equations of a steady-state process model. The concept was based on converting a subset of the steady-state model equations to ordinary differential equations (ODEs), resulting in a differential-algebraic equation (DAE) system with equivalent steady-state solutions.[6]

Flowsheet optimization then relied on a time relaxation-based algorithm,[6] derived from the sequential methods for dynamic optimization of DAE systems, as discussed, for

Correspondence concerning this article should be addressed to M. Baldea at mbaldea@che.utexas.edu.

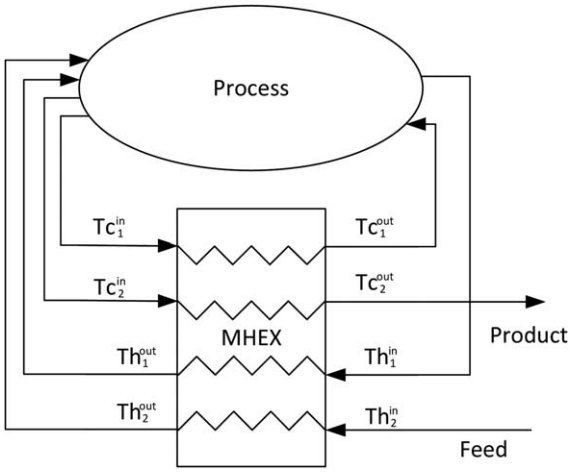

Figure 1. MHEX connected to a process flowsheet.

example, by Vassiliadis et al.[9] Requisite information for the optimization procedure are a set of initial conditions for the differential variables of the DAE system, and initial guesses for the optimization decision variables. The model equations are solved at each iteration by simulating the DAE system to steady state, and then calculating the objective function, constraints, and their gradients. This information is used by the numerical optimization solver to update the decision variables, and again simulate the DAE system to a new steady state. This procedure continues until an optimality criterion is satisfied.[6,10,11] The process is illustrated in Figure 2.

Through proper selection of the transient model parameters, the pseudo-transient solution method has proven to have superior steady-state flowsheet simulation and optimization properties in comparison with existing EO techniques. The framework preserves the advantages of EO flowsheet modeling but vastly expands the set of initial conditions that guarantee the convergence of numerical solution strategies for simulation and optimization.

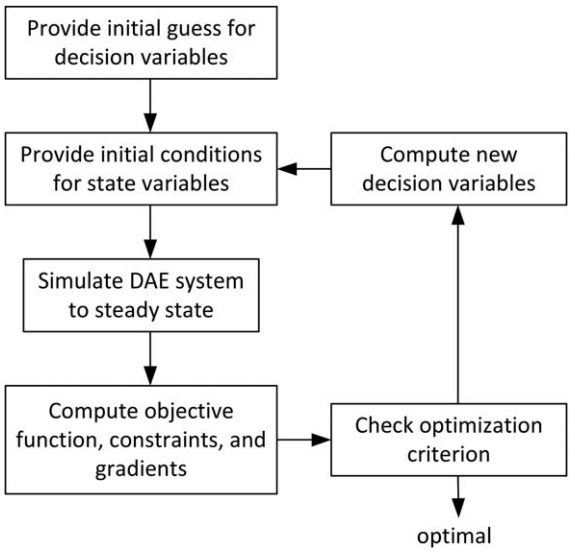

Figure 2. Time relaxation-based optimization algorithm for pseudo-transient models.[6,7]

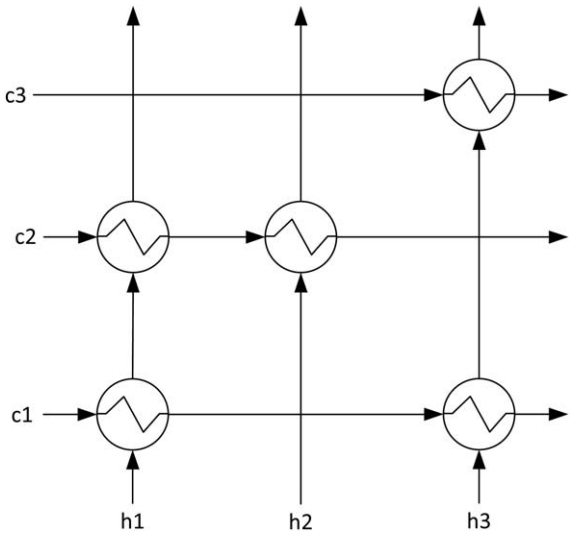

Figure 3. Diagram of a network of two-stream heat exchangers (*c*1, *c*2, *c*3 represent cold streams and *h*1, *h*2, *h*3 represent hot streams).

In this work, we extend the aforementioned pseudo-transient framework to the modeling of MHEXs.

MHEX modeling challenges

To illustrate the challenges of modeling multistream heat exchangers, let us begin by considering a network of two-stream heat exchangers (Figure 3) in a process where constant heat capacity is assumed.[2] Each heat exchanger can be modeled by

$$F_h(T_h^{\text{in}}-T_h^{\text{out}})=F_c(T_c^{\text{out}}-T_c^{\text{in}}) \tag{1}$$

$$T_h^{\text{in}} \geq T_c^{\text{out}}+\Delta T_{\min} \tag{2}$$

$$T_h^{\text{out}} \geq T_c^{\text{in}}+\Delta T_{\min} \tag{3}$$

where index $c \in C$ represents the set of cold streams, index $h \in H$ represents the set of hot streams, and F is the temperature-independent product of heat capacity and flow rate. The pinch (the point along the heat exchanger where the temperature driving force is at a minimum) for the two-stream heat exchangers will occur at the inlet or outlet of the heat exchanger, making the minimum approach temperature constraints (2, 3) relatively easy to enforce. Extending the energy balance to the MHEX case is straightforward

$$\sum_h F_h(T_h^{\text{in}}-T_h^{\text{out}})=\sum_c F_c(T_c^{\text{out}}-T_c^{\text{in}}) \tag{4}$$

However, in an MHEX, because multiple hot and cold streams may exchange heat simultaneously, the minimum temperature approach constraints between any two streams cannot be written explicitly in terms of the inlet and outlet stream temperatures (i.e., an equivalent set of constraints (2, 3) cannot be enforced for an MHEX). Furthermore, the temperature driving forces are typically very small in MHEXs (typically 1–3°C[12]), and assuming constant heat capacities over wide temperature ranges may be inadequate.

Additional complications arise when phase transitions occur in one or more of the process streams within the MHEX. Enthalpy is a piecewise continuous function of

temperature and is calculated as a function of the stream phase as

$$H_{\mathrm{pp}}\Big(T,P,F,x) = \begin{cases} H^{\mathrm{L}}(T,P,F,x) & T \le T_{\mathrm{bub}} \\ H^{\mathrm{2p}}(T,P,F,x) & T_{\mathrm{bub}} < T < T_{\mathrm{dew}} \\ H^{\mathrm{V}}(T,P,F,x) & T \ge T_{\mathrm{dew}} \end{cases} \quad (5)$$

where T, P, F, and x are, respectively, the temperature, pressure, composition, and flow rate of the process streams, the superscripts L, 2p, and V denote the liquid, two-phase, and vapor regimes, and T_{bub} and T_{dew} are, respectively, the dew and bubble points of the fluid.

In the case of simulating the heat exchanger, the stream phases at the inlet of, or within the MHEX may not be known *a priori*. Furthermore, in the context of flowsheet simulation and optimization, the pressures, temperatures, compositions, and flow rates of the MHEX process streams may determined in upstream or downstream process units. Also, the phase boundaries (bubble point and dew point), which must be calculated to detect phase changes, are dependent on stream composition and pressure.

In this work, we will assume that a physical property package is available to compute properties such as stream enthalpy as a function of the temperature, pressure, composition, and flow rate of the process streams, as well as the relevant derivatives. We note that such capability is available in several commercial software packages, which confirms that our assumption is reasonable.

Openly available literature references on equation-based, optimization-oriented modeling of MHEXs are limited. Several contributions focused on optimal design of HENs with process streams that change phase. Ponce-Ortega et al.[13] proposed an MINLP formulation that is an extension of the work by Yee et al.[3] to optimize HENs with isothermal streams, but multicomponent streams undergoing phase change are not considered (see also Ref. 14). Hasan et al.[15] provide a methodology for the optimal design of HENs with multicomponent streams with phase change, but assume that the inlet and outlet stream states are fixed at the design stage and cannot vary.

More recently, several efforts have focused specifically on developing MHEX models amenable to EO flowsheet optimization. An extension of the seminal heat integration approach of Duran and Grossman[2] was introduced by Dowling and Biegler[16]; MHEXs are modeled by individual heat exchangers in series, having distinct phases and using piecewise constant approximations of the temperature-dependence of heat capacity. Kamath et al.[17] similarly proposed an extension of the Duran and Grossmann model[2] that uses a disjunctive programming-based formulation to capture the effect of phase changes. The method relies on a decomposition of the streams into sets of substreams that account for all the possible phases (vapor, liquid, and two-phase); an optimization subproblem involving binary variables is solved to select the proper phase.

To date, the development of an MHEX modeling framework that (1) can capture phase transformations for streams with arbitrary inlet compositions and temperatures, (2) can provide an estimate of heat exchange area for cost estimation, and (3) is amenable to use in the context of flowsheet optimization, remains an open research problem.

In the next section, we provide a novel solution to this problem. In particular, we exploit the pseudo-transient modeling ideas introduced in our previous work[6] to develop a new MHEX model structure and simulation strategy, and subsequently integrate these developments in the flowsheet optimization framework described earlier.

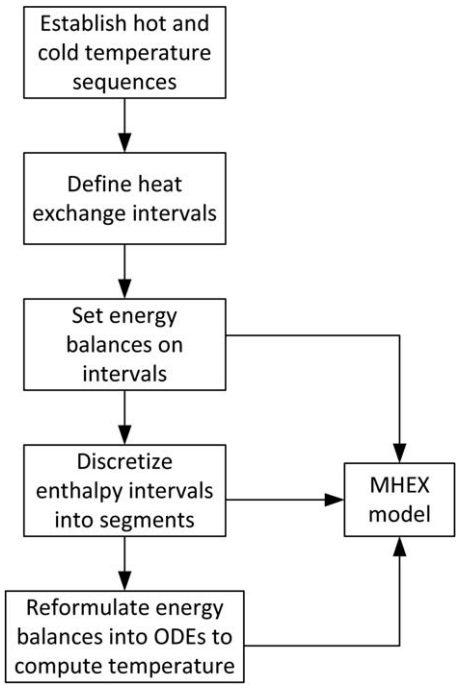

Figure 4. Flowchart of the framework presented for deriving the pseudo-transient MHEX model.

A Pseudo-Transient Framework for EO MHEX Modeling

The energy balance for an MHEX is written in the most general form by considering the enthalpies (H) of the hot and cold streams ($h \in H$ and $c \in C$, respectively)

$$\sum_c (H_c^{\mathrm{out}} - H_c^{\mathrm{in}}) = \sum_h (H_h^{\mathrm{in}} - H_h^{\mathrm{out}}) \quad (6)$$

Note that Eq. 6 is more general than Eq. 4 as it does not restrict the heat capacity of the stream to be temperature-invariant. For design models of MHEXs, the steady-state simulation has a single degree of freedom: the outlet temperature of one of the streams (with the other inlet and outlet temperatures being specified or computed elsewhere in the flowsheet) based on the overall energy balance.

Equation 6 is necessary to simulate the MHEX. However, to determine if the MHEX satisfies the thermodynamic constraint that the minimum approach temperature is not violated along the entire heat exchanger, the temperature of the hot and cold streams must be computed at every point along the heat exchanger. Determining the stream phase at each point in the heat exchanger, selecting the correct branch in (5) to compute the stream temperature, and ensuring the convergence of this calculation are in effect the main challenges of MHEX modeling and simulation.

Our modeling approach consists of four steps, which are shown in Figure 4 and described in detail later.

Throughout the presentation, we will illustrate each step using a simple example comprising two hot streams and two cold streams, with data given in Table 1.

In this simple example, we assume that the inlet and outlet temperatures and flow rates of all streams are known and

Table 1. Motivating Example Parameters

	*C*1	*C*2	*H*1	*H*2
Heat capacity of stream (kW/K)	5	2.6	2	4
Inlet temperature (°C)	40	20	150	180
Outlet temperature (°C)	145 (calculated)	95	40	40

fixed (with the outlet temperature of one stream calculated to satisfy the overall energy balance) and that the MHEX is a standalone unit in the flowsheet. We further assume that the streams do not undergo phase change and that the heat capacity is not temperature dependent. Although these assumptions greatly simplify the problem, the modeling framework presented here is generally applicable without imposing these assumptions, as will be shown in the case studies discussed later in the paper.

Throughout our developments, we will make use of the concept of composite curves.[18] Hot and cold composite curves can be constructed on a temperature-enthalpy plot by considering the cumulative heat transferred on the abscissa and the corresponding temperature of all hot and cold streams on the ordinate (Figure 5). The hot composite curve represents the available heat of the process streams, and the cold composite curve represents the heat demands of the process. The composite curves for the example system are plotted in Figure 5.

Step 1: Construct enthalpy intervals

Concept. The first step in constructing the model for the MHEX is to establish an ordered set of enthalpy intervals. Many HEN optimization models have avoided interval analyses due to the fact that selecting the intervals involves making discrete decisions.[2,17] However, in the present formulation, we are not fixing the intervals; rather, we are fixing only the stream temperature sequence.

Definition 1. *The cold temperature sequence is defined as the order, from coldest to hottest, of the inlet and outlet temperatures of the cold stream set.*

Definition 2. *The hot temperature sequence is defined as the order, from coldest to hottest, of the inlet and outlet temperatures of the hot stream set.*

We assume that the cold and hot temperature sequences are known prior to simulation and optimization, and that the sequence will not change. For example, in the motivating example, the inlet temperature of *C*2 is lower than the inlet temperature of *C*1; if these temperatures are determined in other parts of the flowsheet, or if they are free to vary in a process optimization context, the established sequence of the stream temperatures should not change (i.e., the inlet temperature of *C*2 will always be lower than the inlet temperature of *C*1). Note that for many applications where MHEXs are used (e.g., cryogenic systems), the temperature sequences are typically known prior to flowsheet simulation or optimization. We will address the case when the stream sequences are incorrectly selected later in the article.

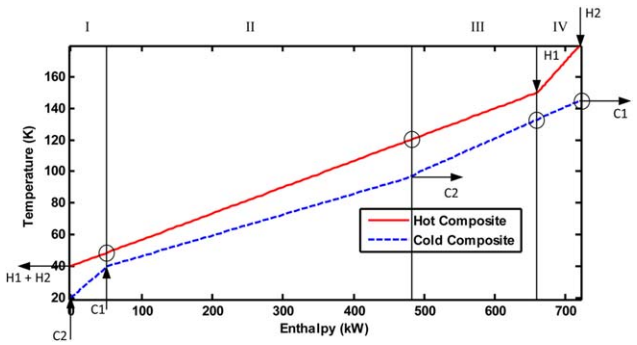

Figure 5. Hot and cold composite curves on the temperature-enthalpy diagram for the motivating example.

[Color figure can be viewed in the online issue, which is available at wileyonlinelibrary.com.]

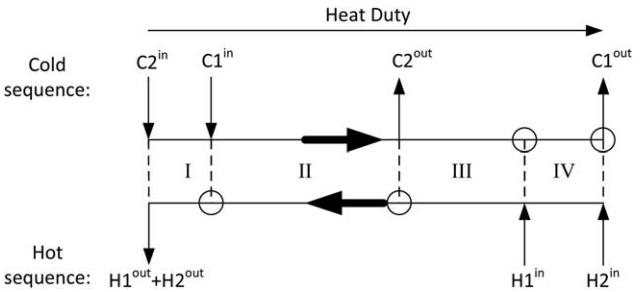

Figure 6. Enthalpy interval chart for the motivating example.

The hot and cold inlet and outlet temperatures are sequenced from coldest to hottest (left to right), and the length between the sequence of points represents an approximation of the required heat duty in the interval. Intervals are numbered using roman numerals.

Definition 3. *An enthalpy interval is defined as the region of the composite curve plot between two consecutive stream feed/exit points.*

To establish the enthalpy intervals, we first identify the cold and hot temperature sequences by ordering the inlet and outlet temperatures from coldest to hottest. Note that an estimation for the calculated stream temperature must be made.

Simple Example (Continued). In our simple example, the cold temperature sequence is: (1) *C*2 inlet, (2) *C*1 inlet, (3) *C*2 outlet, and (4) *C*1 outlet. Likewise, for the hot streams, the temperature sequence is: (1) *H*1 and *H*2 outlet, (2) *H*1 inlet, and (3) *H*2 inlet. These sequences can be visualized on an interval chart as seen in Figure 6, by aligning the lowest temperatures and the hottest temperatures of each sequence. This analysis shows that there are 4 points in the cold temperature sequence ($N_C = 4$), and 3 points in the hot temperature sequence ($N_H = 3$). The number of enthalpy intervals in the MHEX is given by

$$N_{\mathrm{HX}} = N_C + N_H - 3 \tag{7}$$

Thus, the motivating example has four heat exchange intervals which are displayed in Figure 6.

Step 2: Establish energy balances on the enthalpy intervals

Concept. Each enthalpy interval can be treated as a separate heat exchanger where all of the hot streams in the interval exchange heat with all of the cold streams in the interval before exiting. Thus, we can establish energy balances for each interval. The set of interval energy balances forms a linear system of equations where the number of unknowns is equal to the number of intervals. These unknown variables are the enthalpies of the composite curves at the interval boundaries (in case these enthalpies cannot be determined from the properties of inlet or outlet streams). The unknown enthalpies in the motivating example are circled in Figures 5 and 6.

To establish interval-level energy balances, we define the sets of streams (S_i) present in each enthalpy interval ($i \in$ INT), where INT represents the set of all intervals. The energy balances on each interval along with the conditions that ensure continuity of the stream conditions between consecutive intervals form a linear system of equations

$$Q_i = \sum_{c \in S_i} (H^{\text{out}}_{c,i} - H^{\text{in}}_{c,i}) = \sum_{h \in S_i} (H^{\text{in}}_{h,i} - H^{\text{out}}_{h,i}) \tag{8}$$

$$0 = H^{\text{out}}_{c,i} - H^{\text{in}}_{c,i+1} \forall c \in (S_i \cap S_{i+1}) \tag{9}$$

$$0 = H^{\text{in}}_{h,i} - H^{\text{out}}_{h,i+1} \forall h \in (S_i \cap S_{i+1}) \tag{10}$$

where Q_i is the heat duty in each interval.

Simple Example (Continued). In our example, we have $S_{\text{I}} = [C2, H1, H2], S_{\text{II}} = [C1, C2, H1, H2]$, etc., and the interval energy balances are

$$Q_{\text{I}} = H^{\text{out}}_{C2,\text{I}} - H^{\text{in}}_{C2,\text{I}} = (\underline{H^{\text{in}}_{H1,\text{I}} + H^{\text{in}}_{H2,\text{I}}}) - H^{\text{out}}_{H1,\text{I}} - H^{\text{out}}_{H2,\text{I}} \tag{11}$$

$$\begin{aligned} Q_{\text{II}} &= H^{\text{out}}_{C1,\text{II}} + H^{\text{out}}_{C2,\text{II}} - H^{\text{in}}_{C1,\text{II}} - H^{\text{in}}_{C2,\text{II}} \\ &= (\underline{H^{\text{in}}_{H1,\text{II}} + H^{\text{in}}_{H2,\text{II}}}) - (\underline{H^{\text{out}}_{H1,\text{II}} + H^{\text{out}}_{H2,\text{II}}}) \end{aligned} \tag{12}$$

$$Q_{\text{III}} = \underline{H^{\text{out}}_{C1,\text{III}}} - H^{\text{in}}_{C1,\text{III}} = H^{\text{in}}_{H1,\text{III}} + H^{\text{in}}_{H2,\text{III}} - (\underline{H^{\text{out}}_{H1,\text{III}} + H^{\text{out}}_{H2,\text{III}}}) \tag{13}$$

$$Q_{\text{IV}} = \underline{H^{\text{out}}_{C1,\text{IV}}} - \underline{H^{\text{in}}_{C1,\text{IV}}} = H^{\text{in}}_{H2,\text{IV}} - H^{\text{out}}_{H2,\text{IV}} \tag{14}$$

where the underlined (summation) variables represent the unknown enthalpies of the composite curves. We redefine these underlined quantities as X_1, X_2, X_3, X_4

$$X_1 = H^{\text{in}}_{H1,\text{I}} + H^{\text{in}}_{H2,\text{I}} = H^{\text{out}}_{H1,\text{II}} + H^{\text{out}}_{H2,\text{II}} \tag{15}$$

$$X_2 = H^{\text{in}}_{H1,\text{II}} + H^{\text{in}}_{H2,\text{II}} = H^{\text{out}}_{H1,\text{III}} + H^{\text{out}}_{H2,\text{III}} \tag{16}$$

$$X_3 = H^{\text{out}}_{C1,\text{III}} = H^{\text{in}}_{C1,\text{IV}} \tag{17}$$

$$X_4 = H^{\text{out}}_{C1,\text{IV}} \tag{18}$$

and the conditions ensuring continuity between consecutive intervals are given by

$$0 = H^{\text{in}}_{C2,\text{II}} - H^{E}_{C2,\text{I}} \tag{19}$$

$$0 = H^{\text{in}}_{C1,\text{III}} - H^{\text{out}}_{C1,\text{II}} \tag{20}$$

$$0 = H^{\text{in}}_{H1,\text{III}} - H^{\text{out}}_{H1,\text{IV}} \tag{21}$$

The resulting energy balances after making the appropriate substitutions is given by the linear system

$$Q_{\text{I}} = H^{\text{in}}_{C2,\text{II}} - H^{\text{in}}_{C2,\text{I}} = X_1 - H^{\text{out}}_{H1,\text{I}} - H^{\text{out}}_{H2,\text{I}} \tag{22}$$

$$Q_{\text{II}} = H^{\text{out}}_{C1,\text{II}} + H^{\text{out}}_{C2,\text{II}} - H^{\text{in}}_{C1,\text{II}} - H^{\text{in}}_{C2,\text{II}} = X_2 - X_1 \tag{23}$$

$$Q_{\text{III}} = X_3 - H^{\text{out}}_{C1,\text{II}} = H^{\text{out}}_{H1,\text{IV}} + H^{\text{in}}_{H2,\text{III}} - X_2 \tag{24}$$

$$Q_{\text{IV}} = X_4 - X_3 = H^{\text{in}}_{H2,\text{IV}} - H^{\text{out}}_{H2,\text{IV}} \tag{25}$$

The solution of this linear system provides the enthalpy of each composite curve at every interval boundary.

Step 3: Discretize the enthalpy intervals

Concept. To ensure that the MHEX operation is thermodynamically feasible and the temperature driving force is above the minimum approach temperature at every point of the heat exchanger, the temperature-dependence of the heat capacities and the possibility for phase change must be taken into account. Therefore, the heat duty in each enthalpy interval is discretized further into enthalpy segments (see Figure 7).

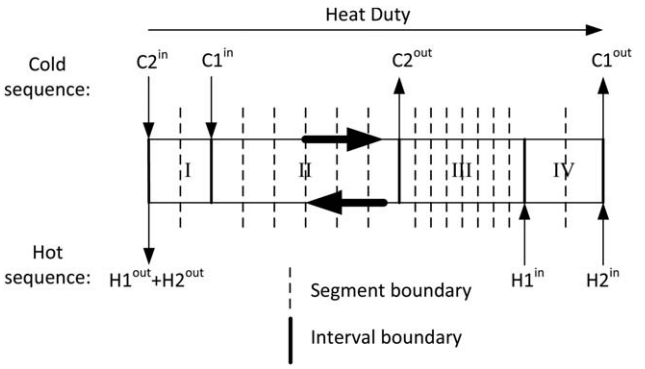

Figure 7. Segmentation of the enthalpy intervals into heat duty segments on the interval diagram for the motivating example.

Notice that the segments have uniform width in each interval, but the number of segments (and segment width) can vary between intervals.

The number of segments necessary to accurately describe the temperature-enthalpy composite curves within each enthalpy interval depends on the degree to which the heat capacity changes with temperature and the likelihood of streams undergoing phase change within that interval. Intuitively, if there is a strong temperature dependence and the temperatures in the interval vary over a wide range, more segments should be used. The number of segments in each interval, $i \in$ INT, is given by N_i.

The enthalpy of the cold and hot composite curves (Hc_i and Hh_i) at each discrete heat duty segment ($z_i = [0, 1, 2, ..., N_i]$) along each enthalpy interval i is given by

$$Hc_i(z_i) = \frac{Q_i}{N_i}(z_i) + \sum_{c \in S_i} H^{\text{in}}_{c,i} \tag{26}$$

$$Hh_i(z_i) = \frac{Q_i}{N_i}(z_i) + \sum_{h \in S_i} H^{\text{out}}_{h,i} \tag{27}$$

Simple Example (Continued). We select $N_{\text{I}} = 2$, $N_{\text{II}} = 10$, $N_{\text{III}} = 5$, and $N_{\text{IV}} = 2$; this results in $z_{\text{I}} = [0, 1, 2]$, $z_{\text{II}} = [0, 1, ..., 10]$, etc. The enthalpy of the cold composite curve at every discrete point in each interval is given by

$$Hc_{\text{I}}(z_{\text{I}}) = \frac{Q_{\text{I}}}{2}(z_{\text{I}}) + H^{\text{in}}_{C2,\text{I}} \tag{28}$$

$$Hc_{\text{II}}(z_{\text{II}}) = \frac{Q_{\text{II}}}{10}(z_{\text{II}}) + H^{\text{in}}_{C1,\text{II}} + H^{\text{in}}_{C2,\text{II}} \tag{29}$$

$$Hc_{\text{III}}(z_{\text{III}}) = \frac{Q_{\text{III}}}{5}(z_{\text{III}}) + H^{\text{in}}_{C1,\text{III}} \tag{30}$$

$$Hc_{\text{IV}}(z_{\text{IV}}) = \frac{Q_{\text{IV}}}{2}(z_{\text{IV}}) + H^{\text{in}}_{C1,\text{IV}} \tag{31}$$

and likewise, the enthalpy of the hot composite curve at every discrete point in each interval is given by

$$Hh_{\text{I}}(z_{\text{I}}) = \frac{Q_{\text{I}}}{2}(z_{\text{I}}) + H^{\text{out}}_{H1,\text{I}} + H^{\text{out}}_{H2,\text{I}} \tag{32}$$

$$Hh_{\text{II}}(z_{\text{II}}) = \frac{Q_{\text{II}}}{10}(z_{\text{II}}) + H^{\text{out}}_{H1,\text{II}} + H^{\text{out}}_{H2,\text{II}} \tag{33}$$

$$Hh_{\mathrm{III}}(z_{\mathrm{III}}) = \frac{Q_{\mathrm{III}}}{5}(z_{\mathrm{III}}) + H^{\mathrm{out}}_{H1,\mathrm{III}} + H^{\mathrm{out}}_{H2,\mathrm{III}} \tag{34}$$

$$Hh_{\mathrm{IV}}(z_{\mathrm{IV}}) = \frac{Q_{\mathrm{IV}}}{2}(z_{\mathrm{IV}}) + H^{\mathrm{out}}_{H1,\mathrm{IV}} \tag{35}$$

Step 4: Compute stream temperatures

Concept. The key aspect of the model is calculating stream temperatures from enthalpy to ensure that the minimum temperature approach constraints are satisfied along the entire heat exchanger. Equations 8–10, 26, and 27 are all linear, and define the enthalpy of the composite curves at each point along the heat exchanger. The composite curve temperatures ($Tc(z_i)$ and $Th(z_i)$) must be computed by equating the enthalpy determined by the energy balances and the enthalpy computed by the physical properties package

$$Hc_i(z_i) = \sum_{c \in S_i} H_{\mathrm{pp}}(Tc(z_i), P_c(z_i), F_c, x_c) \tag{36}$$

$$Hh_i(z_i) = \sum_{h \in S_i} H_{\mathrm{pp}}(Th(z_i), P_h(z_i), F_h, x_h) \tag{37}$$

Recall that H_{pp}, the enthalpy correlation computed by the physical properties package, is a piecewise function of temperature (see Eq. 5). Computing temperature from enthalpy is challenging because it is a piecewise, nonlinear, and implicit function of enthalpy, pressure, composition, and flow rate. If the phase of each stream at each segment is not known *a priori*, a conventional Newton-type solver is likely to fail in computing the temperature.

To solve Eqs. 36 and 37 for temperature, we propose a novel approach based on pseudo-transient continuation.[19] The concept is to reformulate the equations to ODEs that have the same steady-state solution as the original equations. The "dynamics," which are of the first order and whose evolution in time is driven by the residual of Eqs. 36 and 37, have no physical significance, but are rather a mathematical device to aid in solving for the steady-state temperatures of the composite streams. The reformulated equations are

$$\left(\frac{H_{\mathrm{ref}}}{Tc^0}\right)\tau\frac{dTc(z_i)}{dt} = Hc_i(z_i) - \sum_{c \in S_i} H^{\mathrm{pp}}_c(Tc(z_i), P_c(z_i), F_c, x_c) \tag{38}$$

$$\left(\frac{H_{\mathrm{ref}}}{Th^0}\right)\tau\frac{dTh(z_i)}{dt} = Hh_i(z_i) - \sum_{h \in S_i} H^{\mathrm{pp}}_h(Th(z_i), P_h(z_i), F_h, x_h) \tag{39}$$

where $\frac{H_{\mathrm{ref}}}{T^0}$ is a scaling factor to ensure that the units are consistent and τ is a prescribed (arbitrary) time constant. Rather than providing an initial guess for the temperature and phase of each stream in every segment and solving for temperature via Newton's method, the equations are solved by providing initial conditions for temperature at each segment, then simulating the ODEs to steady state. The initial temperature profiles can simply be constant

$$Tc(z_i) = Tc^0 \tag{40}$$

$$Th(z_i) = Th^0 \tag{41}$$

Note that the steady-state solution of Eqs. 38 and 39 is the same as the solution to the original set of Eqs. 36 and 37.

The method is robust in computing the composite curve temperatures if the system (38, 39) is stable. It is important to note that enthalpy is a globally (nonstrictly) increasing function of temperature (i.e., as the temperature increases, enthalpy increases or is unchanged). Due to the negative weighting on H_{pp}, the ODEs (Eqs. 38 and 39) have negative, and therefore stable, eigenvalues. An example is discussed in Figure 8.

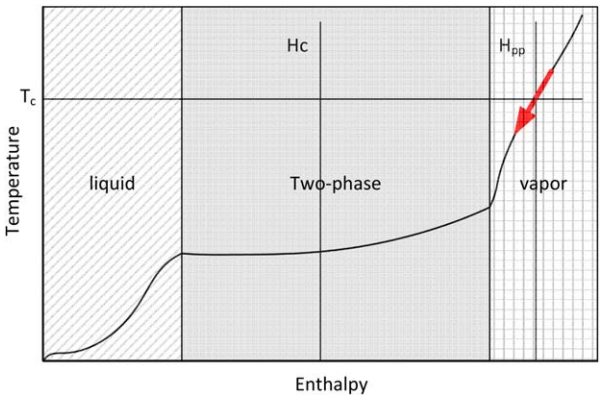

Figure 8. In this example, the enthalpy of the cold composite curve at one point along the heat exchanger (*Hc*) starts being much lower than the enthalpy computed by the physical properties package at the current temperature (H_{pp} and *Tc*, respectively).

This results in the right-hand side in Eq. 38 being negative, and a negative pseudotime derivative for temperature. As the simulation progresses, the temperature will decrease along with the computed enthalpy. At steady state, *Hc* and H_{pp} will be equal, and the steady-state temperature has been found. [Color figure can be viewed in the online issue, which is available at wileyonlinelibrary.com.]

Remark 1. *In our previous work,*[6] *we discussed in detail the selection of the time constants, τ. The time variable does not have physical meaning, and when implemented with a variable step DAE solver, only the relative values of the time constants at different levels of the flowsheet (i.e., phenomenon, unit operation, flowsheet) are relevant. For the case of MHEX, we suggest selecting τ to be in the fastest time scale (phenomenon) as described in the previous work.*

Simple Example (Continued). For the motivating example, the pseudo-transient energy balance equations for the cold composite curve are

$$\left(\frac{H_{\mathrm{ref}}}{Tc^0}\right)\tau\frac{dTc(z_{\mathrm{I}})}{dt} = Hc_{\mathrm{I}}(z_{\mathrm{I}}) - H^{\mathrm{pp}}_{C2}(Tc(z_{\mathrm{I}}), P_{C2}(z_{\mathrm{I}}), F_{C2}, x_{C2}) \tag{42}$$

$$\left(\frac{H_{\mathrm{ref}}}{Tc^0}\right)\tau\frac{dTc(z_{\mathrm{II}})}{dt} = Hc_{\mathrm{II}}(z_{\mathrm{II}}) - H^{\mathrm{pp}}_{C1}(Tc(z_{\mathrm{II}}), P_{C1}(z_{\mathrm{II}}), F_{C1}, x_{C1}) \tag{43}$$

$$- H^{\mathrm{pp}}_{C2}(Tc(z_{\mathrm{II}}), P_{C2}(z_{\mathrm{II}}), F_{C2}, x_{C2}) \tag{44}$$

$$\left(\frac{H_{\mathrm{ref}}}{Tc^0}\right)\tau\frac{dTc(z_{\mathrm{III}})}{dt} = Hc_{\mathrm{III}}(z_{\mathrm{III}}) - H^{\mathrm{pp}}_{C1}(Tc(z_{\mathrm{III}}), P_{C1}(z_{\mathrm{III}}), F_{C1}, x_{C1}) \tag{45}$$

$$\left(\frac{H_{\mathrm{ref}}}{Tc^0}\right)\tau\frac{dTc(z_{\mathrm{IV}})}{dt} = Hc_{\mathrm{IV}}(z_{\mathrm{IV}}) - H^{\mathrm{pp}}_{C1}(Tc(z_{\mathrm{IV}}), P_{C1}(z_{\mathrm{IV}}), F_{C1}, x_{C1}) \tag{46}$$

Likewise, for the hot composite curve, the temperature dynamics are

$$\left(\frac{H_{\text{ref}}}{Th^0}\right)\tau\frac{dTh(z_{\text{I}})}{dt}=Hh_{\text{I}}(z_{\text{I}})-H^{\text{pp}}_{H1}(Th(z_{\text{I}}),P_{H1}(z_{\text{I}}),F_{H1},x_{H1}) \tag{47}$$

$$-H^{\text{pp}}_{H2}(Th(z_{\text{I}}),P_{H2}(z_{\text{I}}),F_{H2},x_{H2}) \tag{48}$$

$$\left(\frac{H_{\text{ref}}}{Th^0}\right)\tau\frac{dTh(z_{\text{II}})}{dt}=Hh_{\text{II}}(z_{\text{II}})-H^{\text{pp}}_{H1}(Th(z_{\text{II}}),P_{H1}(z_{\text{II}}),F_{H1},x_{H1}) \tag{49}$$

$$-H^{\text{pp}}_{H2}(Th(z_{\text{II}}),P_{H2}(z_{\text{II}}),F_{H2},x_{H2}) \tag{50}$$

$$\left(\frac{H_{\text{ref}}}{Th^0}\right)\tau\frac{dTh(z_{\text{III}})}{dt}=Hh_{\text{III}}(z_{\text{III}})-H^{\text{pp}}_{H1}(Th(z_{\text{III}}),P_{H1}(z_{\text{III}}),F_{H1},x_{H1}) \tag{51}$$

$$-H^{\text{pp}}_{H2}(Th(z_{\text{III}}),P_{H2}(z_{\text{III}}),F_{H2},x_{H2}) \tag{52}$$

$$\left(\frac{H_{\text{ref}}}{Th^0}\right)\tau\frac{dTh(z_{\text{IV}})}{dt}=Hh_{\text{IV}}(z_{\text{IV}})-H^{\text{pp}}_{H2}(Th(z_{\text{IV}}),P_{H2}(z_{\text{IV}}),F_{H2},x_{H2}) \tag{53}$$

Initial conditions are provided

$$Tc^0(z_i)=20^\circ\text{C} \tag{54}$$

$$Th^0(z_i)=180^\circ\text{C} \tag{55}$$

The steady state resulting temperatures along the heat exchanger are plotted in the temperature-enthalpy plot (see Figure 5).

Solution strategy

Simulation of the described MHEX model involves solving the linear algebraic equations for enthalpy at each discrete heat duty segment and finding the temperature trajectories from the initial conditions to the steady state. The resulting system is thus a DAE system. We assume that a robust DAE simulation package is available to solve the equations. The DAE simulator should be capable of (1) initializing the algebraic equations, (2) integrating the system through time using a variable time stepping routine, and (3) handle implicit discontinuities encountered during the simulation (e.g., changing phase regimes).

If a phase boundary is encountered during the time integration (e.g., the temperature reduces from superheated to the dew point), an implicit discontinuity will be detected by the DAE solver. From a numerical simulation perspective, this requires a reinitialization of the corresponding DAE system which proceeds by assuming that the state variables (temperature) are continuous through the discontinuity (i.e., $T(t^-)=T(t^+)$, where t^- and t^+ are the time instants immediately prior and, respectively, immediately following the discontinuity. The algebraic variables (in this case the enthalpies, compositions, etc.) are reinitialized (i.e., the linear equations determining the composite curve enthalpies at each point must be resolved) at t^+, using the values prior to the discontinuity as an initial guess. Typically, the reinitialization is fast because the algebraic variables involved here do not change significantly when the phase boundaries are crossed.

Flowsheet Optimization

We note here that the simulation strategy above integrates seamlessly with the pseudo-transient flowsheet optimization framework that we described in our previous work.[6] This will be further emphasized in the case studies presented later.

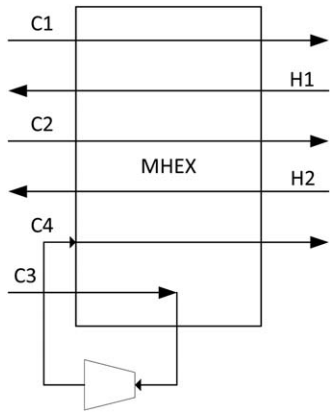

Figure 9. Flowsheet of a hypothetical MHEX representative of ASU operation.

In the case of optimizing flowsheet with MHEXs, several additional constraints must be enforced. To ensure that the net quantity of heat exchanged in each enthalpy interval is positive, Eq. 56 is enforced for each enthalpy interval

$$Q_i \geq 0 \;\; \forall i \in \text{INT} \tag{56}$$

Remark 2. *An active constraint (56) at the optimal point, or a violation of constraint (56) which renders the problem infeasible, may indicate that the enthalpy intervals were not established properly. In this case, the temperature sequences should be realigned by switching the order of the two temperatures which bound the interval i that corresponds to the active constraint.*

Additionally, minimum temperature approach constraints must be enforced at every discrete heat duty segment

$$Th(z_i)-Tc(z_i) \geq \Delta T_{\min} \;\; \forall i \in \text{INT} \tag{57}$$

If a higher fidelity composite curve is required to further capture variability in the heat capacities in one or more intervals, the system can be reoptimized using a finer segmentation in the intervals.

Estimating capital cost

In most literature studies regarding design of MHEXs, the capital investment of the heat exchanger cannot be approximated or optimized because only one side of the heat exchanger is accounted for in the model.[2,16,17] In this work, both the hot and cold composite curves are considered, and an approximation of the heat exchanger design requirements (the product of area and heat-transfer coefficient) can be made using the required heat duty and the average temperature driving force along the heat exchanger.

Assuming an approximate heat-transfer coefficient, U_i, the area in every interval can be approximated by averaging the temperature difference in every segment

$$A_i=\frac{Q_i}{U_i}\sum_{z_i}\frac{1}{Th(z_i)-Tc(z_i)} \tag{58}$$

and the total area of the heat exchanger is given by

$$A_{\text{HX}}=\sum_i A_i \tag{59}$$

which can then be used in a cost function to determine the capital investment for the MHEX.

Table 2. Case Study I

	*C*1	*C*2	*C*3	*C*4	*H*1	*H*2
Flow rate (mol/s)	600	variable	variable	variable	800	300
Inlet temperature (K)	94.2	94.2	98.5	98.5	298.15	100
Outlet temperature (K)	293.15	130	variable	293.15	variable	variable
Pressure (bar)	1	5	7	1	8	7
Composition (mol frac)						
N_2	5%	98%	99.9%	99.9%	78%	99.0%
O_2	94.5%	1.9%	0.1%	0.1%	21%	0.1%
Ar	0.5%	0.1%	0.0%	0.0%	1.0%	0.0%

Pressure drop

In the case of MHEXs, the pressure drop along the heat exchanger is typically assumed by the designer, and it is often considered to vary linearly with heat duty. For example, the pressure drop can be calculated (for the cold and hot streams, respectively), using correlations of the form

$$P_{c,i}(z_i)=P_{c,i}^{\text{in}}-\frac{\delta P_{c,i}}{N_i}(z_i) \tag{60}$$

$$P_{h,i}(z_i)=P_{h,i}^{\text{in}}-\delta P_{h,i}\left(1-\frac{z_i}{N_i}\right) \tag{61}$$

$$\delta P_{c,i}=\frac{Q_i}{\sum_{i:c\in S_i} Q_i}\Delta P_c \tag{62}$$

$$\delta P_{h,i}=\frac{Q_i}{\sum_{i:h\in S_i} Q_i}\Delta P_h \tag{63}$$

which can be easily added to our model.

Examples

Two case examples are explored to demonstrate the capabilities of the proposed MHEX model in EO flowsheet optimization. The first example ignores the majority of the flowsheet and focuses on simply optimizing a hypothetical MHEX representative of an air separation unit (ASU). The second is an industrial natural gas liquefaction process. In both cases, the mathematical models were implemented and solved using gPROMS.[20]

MHEX representative of ASU operation

The first case study is a very simple flowsheet with only an MHEX and a turbine expander that is representative of ASU operation (see Figure 9). MHEXs are critical for heat integration and refrigeration recovery in ASUs (Cao et al. submitted).[17,21] In this case, we consider an MHEX with four hot streams and two cold streams, with the properties (temperature, pressure, and composition) of some of the process streams being decision variables in the optimization. The stream data are given in Table 2. An impure oxygen stream (*C*1) enters the MHEX at the same temperature as a liquid nitrogen stream (*C*2) at the bubble point. A pure nitrogen gas stream (*C*3) at the dew point also partially passes through the MHEX; the outlet of this stream is expanded to 1 bar and repassed through the MHEX (*C*4) at the same temperature as *C*3. The exit temperature of *C*3 is calculated based on the pressure drop in the turbine expander assuming 80% isentropic efficiency. An air stream (*H*1) enters at 25°C and is cooled and liquefied along with a high-pressure nitrogen stream (*H*2) which enters at −167°C that is also liquefied in the MHEX. It is assumed that the pressure drop is negligible for each stream.

Two design objectives are investigated, the first seeks to use a minimum amount of liquid and gas nitrogen (where liquid is four times as costly as gas) to liquefy the incoming air stream and the nitrogen gas stream. The second objective is equivalent, but includes a penalty for the required area of the heat exchanger. The single degree of freedom on the MHEX is the exit temperature of the air stream; this temperature is constrained to a maximum of 99 K. The minimum approach temperature is 2°C, and the Soave–Redlich–Kwong (SRK) cubic equation of state is used to model the physical properties. The optimization problem formulation for objective 2 is given by (64), where we assume a penalty for the heat exchanger area ($c = 500$) (for objective 1, we set $c = 0$)

$$\begin{aligned} \min_{F_{C2},F_{C3}} \quad & J=4F_{C2}+F_{C3}+cA_{\text{HX}} & \\ \text{s.t.} \quad & Q_i \geq 0 & \forall i \in \text{INT} \\ & Th(z_i)-Tc(z_i) \geq \Delta T_{\min} & \forall i \in \text{INT} \\ & \text{model equations} & \end{aligned} \tag{64}$$

Pseudo-transient models of the turbine and the MHEX are used to simulate and optimize the flowsheet. The first step in modeling the MHEX is to construct the enthalpy intervals. To do this, we first determine the cold and hot stream temperature sequences (see Figure 10). The cold stream sequence is: (1) *C*1 and *C*2 inlet, (2) *C*3 and *C*4 inlet, (3) *C*2 outlet, (4) *C*3 outlet, and (5) *C*1 and *C*4 outlet. The hot stream sequence is: (1) *H*1 and *H*2 outlet, (2) *H*2 inlet, and (3) *H*1 inlet. The cold sequence has 5 points ($N_C = 5$) and the hot sequence has 3 points ($N_H = 3$). This results in five enthalpy intervals in the MHEX ($N_{\text{HX}}=N_C+N_H-3=5$). The five intervals are shown in Figure 10.

The steps in the previous section are followed to generate a pseudo-transient model of the MHEX and the turbine. Each of the five enthalpy intervals are discretized into five segments to account for phase change and temperature-dependent heat capacities.

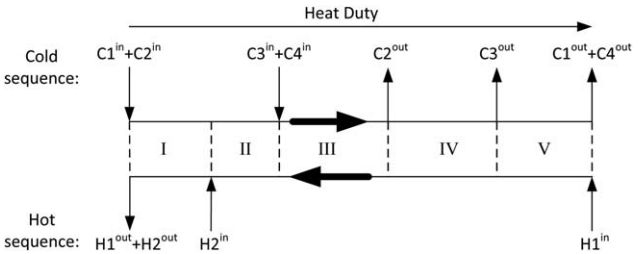

Figure 10. The temperature sequence of the hot and cold composite curves for case study I.

The assumed enthalpy intervals are shown with the vertical lines (I–V).

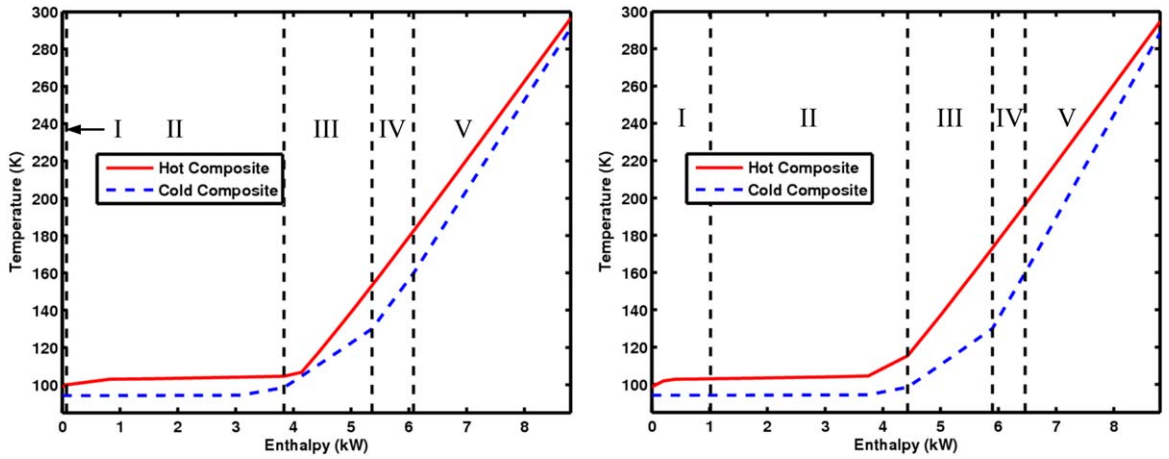

Figure 11. Optimal temperature-enthalpy diagrams for the MHEX in an air separation process for objective functions 1 (left) and 2 (right).

The interval boundaries are superimposed on the figure by the vertical black lines. [Color figure can be viewed in the online issue, which is available at wileyonlinelibrary.com.]

The optimum using the first objective function (not including capital costs) uses 746.9 mol/s of liquid nitrogen (*C*2) and 108.2 mol/s of nitrogen gas (*C*3 and *C*4). The optimum found using the second objective function indicates a flow rate of liquid nitrogen of 864.2 mol/s and a flow rate of nitrogen gas of 22.0 mol/s. The optimization selects to use more liquid nitrogen to maintain a higher driving force and consequently require less surface area. The outlet temperature of the air stream at the optimal point is 99 K for both cases, and the minimum approach temperature is 2°C, thus satisfying the respective constraints. The hot and cold composite curves at the optimum are shown in Figures 11a, b for objectives 1 and 2, respectively, along with the superimposed interval boundaries. The majority of the heat is exchanged in interval II, where the liquid nitrogen (stream *C*2) is evaporated and the air and nitrogen streams (*H*1 and *H*2, respectively) are liquefied. Notice that in the case where the area of the heat exchanger is penalized, the temperature driving force along the heat exchanger is higher (i.e., the vertical distance between the hot and cold composite curves is larger). Another important aspect of this MHEX modeling framework is that there are not dedicated "phase change" intervals. In intervals I and II, both hot streams transition from gas phase to two-phase to liquid phase, and the cold stream *C*2 transitions from liquid phase to two-phase to gas phase. The other streams are single-phase, and none of the phase transitions occur at the interval boundaries. The optimal solution was found in 12.1 s and 11.2 s for objective functions 1 and 2, respectively, on a 64-bit Windows 7 desktop system with a 3.40GHz Intel Core i7 processor and 16 GB of RAM.

Case study: PRICO® liquefaction process

The PRICO® (PRICO® is a registered service mark of Black & Veatch holding company) process for natural gas liquefaction makes use of an MHEX for cooling and liquefying natural gas.[17,22,23] The process flow diagram is given in Figure 12. The natural gas stream, with a composition of 89.7% methane, 5.5% ethane, 1.8% propane, 0.1% *n*-butane, and 2.8% nitrogen, enters the MHEX at 25°C and 55 bar with a flow rate of 1 kmol/s and is liquefied and subcooled to −155°C. The natural gas stream is cooled by a mixed refrigerant of nitrogen, methane, ethane, propane, and butane in a single-stage refrigeration cycle. The mixed refrigerant is cooled in the MHEX, expanded across the throttle valve, repassed through the MHEX to liquefy the natural gas, compressed, then chilled to 25°C in the salt water (SW) cooler.

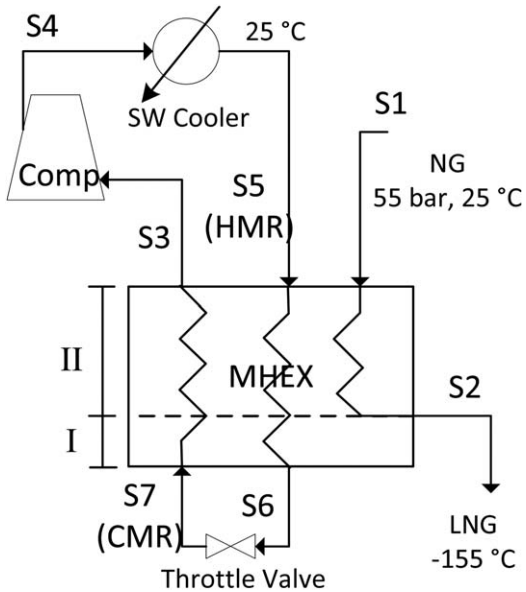

Figure 12. Process flow diagram for the PRICO® liquefaction process.[22]

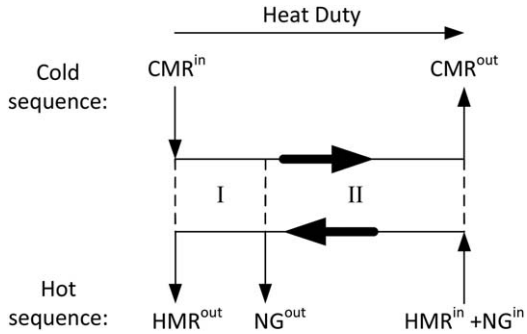

Figure 13. Interval diagram for the PRICO® liquefaction process.

Table 3. PRICO® Optimization Results Comparison

	Nogal et al.[24]	Kamath et al.[17]	This Work
Power (MW)	24.53	21.51	20.00
Pressure *S*3 (bar)	4.84	2.02	3.38
Pressure *S*4 (bar)	43.87	17.129	26.55
MR Flow (kmol/s)	3.53	2.928	2.885
N_2 (mol %)	10.08	5.82	8.81
CH_4 (mol %)	27.12	20.62	32.29
C_2H_6 (mol %)	37.21	39.37	32.79
C_3H_8 (mol %)	0.27	0.0	0.63
$n-C_4H_6$ (mol %)	25.31	34.19	25.48

There is a 5 bar pressure drop for the natural gas stream across the MHEX, a 4 and 1 bar pressure drop for the hot and cold refrigerant streams, respectively, and a 0.1 bar pressure drop across the SW cooler. The compressor is assumed to operate with a fixed isentropic efficiency of 80%, and the SRK cubic equation of state is used to model the thermodynamic properties.

This example poses several challenges during optimization: (1) the phase of the refrigerant stream is unknown: *S*5, *S*6, and *S*7 could be in the liquid phase, vapor phase, or two-phase, (2) the pressures and temperatures of the refrigerant stream are free to vary throughout the process, (3) the composition and flow rate of the refrigerant is free to vary during the optimization resulting in moving phase boundaries, and (4) a very small minimum approach temperature (1.2°C) is required to ensure maximum energy recovery.

Optimization of the PRICO® process consists of minimizing the work done by the compressor, and several recent studies have explored the optimization of this process.[17,24] The decision variables consist of the composition and flow rate of the refrigerant, the high and low pressures in the refrigeration cycle, and the exit temperature of the hot refrigerant (HMR). The single degree of freedom in the MHEX is the exit temperature of the cold refrigerant (CMR) stream. To ensure that the feed to the compressor is in the vapor phase, the CMR outlet temperature must be above the dew point.

We apply the pseudo-transient MHEX modeling methodology to the PRICO® process to simulate and optimize the flowsheet. The first step in modeling the MHEX is to construct the enthalpy intervals. To do this, we first determine the cold and hot stream temperature sequences. The cold stream sequence is: (1) CMR inlet and (2) CMR outlet. The hot stream sequence is: (1) HMR outlet, (2) NG outlet, and (3) HMR and NG inlets. The cold sequence has 2 points ($N_C = 2$) and the hot sequence has 3 points ($N_H = 3$). This results in two enthalpy intervals in the MHEX ($N_{HX} = N_C + N_H - 3 = 2$). Intervals I and II are separated by the point at which the natural gas stream exits the heat exchanger. The interval diagram for the MHEX is given in Figure 13.

Each enthalpy interval is discretized further into enthalpy segments to account for nonconstant heat capacities and phase change. A small fraction of the total heat duty will likely be exchanged in interval I, while the majority will be exchanged in interval II; using this knowledge, we select $N_I = 5$ and $N_{II} = 45$. The enthalpies of the composite curves are established at every discrete heat duty point through Eqs. 26 and 27, and the pseudo-transient energy balances to compute temperature are given by Eq. 38 and 39. The pressure of each stream at every segment is determined by Eq. 60−63.

A multistart strategy, where several distant initial guesses were provided that spanned the decision variable bounds, was used to find the best locally optimal solution. The results of the optimization, along with a comparison of the optimal results found in previous works, are presented in Table 3. The optimal solution found in this work uses 18.5% less power than the work by Nogal et al.,[24] and 7.0% less power than the work by Kamath et al.[17] The solution features a lower flow rate of refrigerant compared with the optimal solution found in Kamath et al., but operates at higher pressures. The compression ratio is also lower than in previous published results (9.1 in Nogal et al., 8.5 in Kamath et al., and 7.9 in our work). The hot and cold composite temperature-enthalpy curves at the optimum are displayed in Figure 14; the process shows very tight heat integration as the temperature driving force at every point along the heat exchanger is very small. Similar to the results found in Kamath et al., the outlet of the SW cooler is two-phase, the HMR at the outlet of the MHEX is subcooled, and the CMR at the inlet is two-phase. The CMR at the outlet is superheated to satisfy the constraint that the feed to the compressor must be in the vapor phase. Notice that interval I spans a much smaller heat duty than interval II, as shown by the interval boundary superimposed on Figure 14. The high nonlinearity of the composite curves with respect to temperature is apparent; a constant heat capacity assumption would likely yield deficient results. The optimal solution was found in 117 s using a 64-bit Windows 7 desktop system with a 3.40GHz Intel Core i7 processor and 16 GB of RAM.

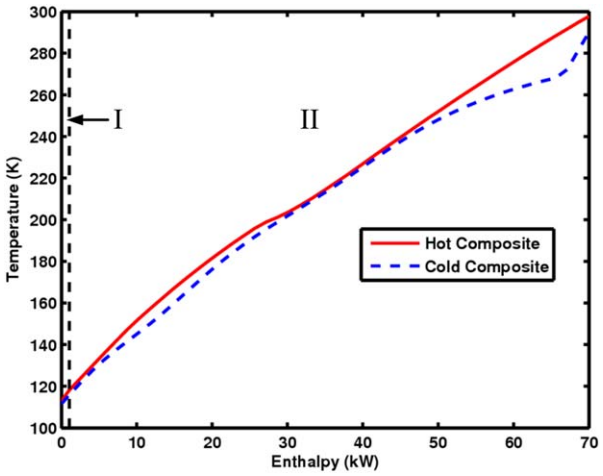

Figure 14. Optimal temperature-enthalpy diagram for the PRICO® liquefaction process.

The interval boundary is given by the vertical line on the left. [Color figure can be viewed in the online issue, which is available at wileyonlinelibrary.com.]

Conclusions

In this work, we present a simple and transparent modeling framework for MHEXs that is amenable to EO flowsheet optimization. Under the assumption that the relative sequence of stream temperatures is known prior to simulation and optimization, the model is able to readily account for phase change without requiring Boolean decisions by discretizing the heat duty and applying a pseudo-transient framework to calculate the stream temperatures from enthalpy along the entire heat exchanger. Furthermore, the model is capable of computing the required heat exchanger area from heat duty and temperature driving force to

determine the optimal tradeoff between capital and operating expenditures.

The model can be incorporated into flowsheet with other pseudo-transient unit operations developed in previous work,[6] and such flowsheet can be optimized using a time relaxation-based optimization algorithm. Several case studies were explored, a standalone MHEX representative of an ASU, as well as the industrial PRICO® liquefaction process.

Acknowledgments

The authors thank the American Chemical Society - Petroleum Research Fund for partial funding under grant 52335-DNI9. RCP gratefully acknowledges the Engineering Doctoral Fellowship awarded to him by the Cockrell School of Engineering at The University of Texas at Austin. MB is also grateful for the support provided by the Moncrief Grand Challenges Award from the Institute for Computational Engineering and Sciences at The University of Texas at Austin.

Notation

F = heat capacity-flow rate, W/K
H = set of hot streams
C = set of cold streams
T = temperature, K
ΔT_{min} = minimum approach temperature, K
P = pressure, Pa
x = composition (mole fraction)
H = enthalpy, W
N_C = cold temperature sequence points
N_H = hot temperature sequence points
N_{HX} = number of heat exchange intervals
S = set of streams in interval
INT = set of intervals
Q = heat exchanged in interval, W
N_i = number of segments in interval
z = segments number in interval
Hc = cold composite curve enthalpy, W
Hh = hot composite curve enthalpy, W
Tc = cold composite curve temperature, K
Th = hot composite curve temperature, K
τ = time constant, s
A_i = required area in interval, m^2
U = heat-transfer coefficient, $W/m^2/K$
A_{HX} = total required area, m^2
ΔP = pressure drop across MHEX, Pa
δP = pressure drop across interval, Pa

Subscripts

c = cold stream
h = hot stream
bub = bubble point
dew = dew point
i = interval

Superscripts

in = stream inlet
out = stream outlet
L = liquid phase
2p = two-phase
V = vapor phase
0 = initial condition

Literature Cited

1. Biegler LT, Grossmann IE, Westerberg AW. *Systematic Methods for Chemical Process Design*. Old Tappan, NJ: Prentice Hall, 1997.
2. Duran MA, Grossmann IE. Simultaneous optimization and heat integration of chemical processes. *AIChE J*. 1986;32(1):123–138.
3. Yee TF, Grossmann IE, Kravanja Z. Simultaneous optimization models for heat integration. I. Area and energy targeting and modeling of multi-stream exchangers. *Comput Chem Eng*. 1990;14(10):1151–1164.
4. Furman KC, Sahinidis NV. A critical review and annotated bibliography for heat exchanger network synthesis in the 20th century. *Ind Eng Chem Res*. 2002;41(10):2335–2370.
5. Hasan MM, Karimi IA, Alfadala HE, Grootjans H. Operational modeling of multistream heat exchangers with phase changes. *AIChE J*. 2009;55(1):150–171.
6. Pattison RC, Baldea M. Equation-oriented flowsheet simulation and optimization using pseudo-transient models. *AIChE J*. 2014;60(12):4104–4123.
7. Pattison RP, Baldea M. Optimal design of air separation plants with variable electricity pricing. *Foundations of Computer-Aided Process Design (FOCAPD)*. Cle Elum, WA: Elsevier, 2014:393–398.
8. Kelley CT, Keyes DE. Convergence analysis of pseudo-transient continuation. *SIAM J Numer Anal*. 1998;35(2):508–523.
9. Vassiliadis VS, Sargent RWH, Pantelides CC. Solution of a class of multistage dynamic optimization problems. I. Problems without path constraints. *Ind Eng Chem Res*. 1994;33(9):2111–2122.
10. Zanfir M, Baldea M, Daoutidis P. Optimizing the catalyst distribution for countercurrent methane steam reforming in plate reactors. *AIChE J*. 2011;57(9):2518–2528.
11. Pattison RC, Estep FE, Baldea M. Pseudodistributed feed configurations for catalytic plate microchannel reactors. *Ind Eng Chem Res*. 2014;53(13):5028–5037.
12. Lee GC, Smith R, Zhu XX. Optimal synthesis of mixed-refrigerant systems for low-temperature processes. *Ind Eng Chem Res*. 2002;41(20):5016–5028.
13. Ponce-Ortega JM, Jiménez-Gutiérrez A, Grossmann IE. Optimal synthesis of heat exchanger networks involving isothermal process streams. *Comput Chem Eng*. 2008;32(8):1918–1942.
14. Grossmann IE, Yeomans H, Kravanja Z. A rigorous disjunctive optimization model for simultaneous flowsheet optimization and heat integration. *Comput Chem Eng*. 1998;22:S157–S164.
15. Hasan MM, Jayaraman G, Karimi IA, Alfadala HE. Synthesis of heat exchanger networks with nonisothermal phase changes. *AIChE J*. 2010;56(4):930–945.
16. Dowling AW, Biegler LT. A framework for efficient large scale equation-oriented flowsheet optimization. *Comput Chem Eng*. 2015;72:3–20.
17. Kamath RS, Biegler LT, Grossmann IE. Modeling multistream heat exchangers with and without phase changes for simultaneous optimization and heat integration. *AIChE J*. 2012;58(1):190–204.
18. Linnhoff B, Flower JR. Synthesis of heat exchanger networks: I. systematic generation of energy optimal networks. *AIChE J*. 1978;24(4):633–642.
19. Coffey TS, Kelley CT, Keyes DE. Pseudo-transient continuation and differential-algebraic equations. *SIAM J Sci Comput*. 2003;25(2):553–569.
20. Process Systems Enterprise. general PROcess Modeling System (gPROMS). Available at: www.psenterprise.com/gproms, 1997–2014.
21. Cao Y, Swartz CLE, Baldea M. Design for dynamic performance: application to an air separation unit. In: *American Control Conference (ACC)*. San Francisco, CA: IEEE, 2011:2683–2688.
22. Price BC, Mortko RA. PRICO: a simple, flexible proven approach to natural gas liquefaction. In: *GASTECH, 17th International LNG/LPG/Natural Gas Conference*. Vienna: RAI, 1996:1–14.
23. Jensen JB, Skogestad S. Optimal operation of a simple LNG process. In: *Proceedings ADCHEM*. Oxford, UK: Elsevier, 2006:241–247.
24. Nogal FD, Kim JK, Perry S, Smith R. Optimal design of mixed refrigerant cycles. *Ind Eng Chem Res*. 2008;47(22):8724–8740.

Manuscript received Dec. 8, 2014, and revision received Feb. 2, 2015.